Available online at www.sciencedirect.com
ScienceDirect
Biochimica et Biophysica Acta 1773 (2007) 1095–1106
Biochimica et Biophysica Acta BBA
www.elsevier.com/locate/bbamcr

Synergistic inhibition of pancreatic adenocarcinoma cell growth by trichostatin A and gemcitabine

Massimo Donadelli [a], Chiara Costanzo [a], Stefania Beghelli [b], Maria Teresa Scupoli [c], Mario Dandrea [a,b], Antonio Bonora [d], Paolo Piacentini [b,1], Alfredo Budillon [e], Michele Caraglia [e], Aldo Scarpa [b,2], Marta Palmieri [a,*,2]

[a] *Department of Morphological and Biomedical Sciences, Section of Biochemistry, University of Verona, Verona, Italy*
[b] *Department of Pathology, University of Verona, Verona, Italy*
[c] *Department of Clinical and Experimental Medicine, Section of Hematology, University of Verona, Verona, Italy*
[d] *Department of Surgical and Gastroenterological Sciences, University of Verona, Verona, Italy*
[e] *Experimental Pharmacology Unit, Experimental Oncology Department, National Institute of Tumours Fondazione G. Pascale, Naples, Italy*

Received 30 January 2007; received in revised form 24 April 2007; accepted 3 May 2007
Available online 22 May 2007

Abstract

We investigated the ability of the histone deacetylase (HDAC) inhibitor trichostatin A (TSA) to interact with gemcitabine (GEM) in inducing pancreatic cancer cell death. The combined treatment with TSA and GEM synergistically inhibited growth of four pancreatic adenocarcinoma cell lines and induced apoptosis. This effect was associated with the induction of reactive oxygen species (ROS) by GEM, increased expression of the pro-apoptotic *BIM* gene by both TSA and GEM and downregulation of the 5′-nucleotidase *UMPH* type II gene by TSA. The expression of other genes critical for GEM resistance (nucleoside transporters, deoxycytidine kinase, cytidine deaminase, and ribonucleotide reductase genes) was not affected by TSA. The functional role of ROS in cell growth inhibition by GEM was supported by (i) a significantly reduced GEM-associated growth inhibition by the free radical scavenger *N*-acetyl-L-cysteine, and (ii) a positive correlation between the basal level of ROS and sensitivity to GEM in 10 pancreatic cancer cell lines. The functional role of both Bim and 5′-nucleotidase UMPH type II in cell growth inhibition by TSA and GEM was assessed by RNA interference assays. *In vivo* studies on xenografts of pancreatic adenocarcinoma cells in nude mice showed that the association of TSA and GEM reduced to 50% the tumour mass and did not cause any apparent form of toxicity, while treatments with TSA or GEM alone were ineffective. In conclusion, the present study demonstrates a potent anti-tumour activity of TSA/GEM combination against pancreatic cancer cells *in vitro* and *in vivo*, strongly supporting the use of GEM in combination with an HDAC inhibitor for pancreatic cancer therapy.

Keywords: Pancreatic cancer; Trichostatin A; Gemcitabine; Apoptosis; Oxidative stress; RNA interference

1. Introduction

Pancreatic adenocarcinoma is one of the most aggressive human cancers. Its incidence nearly mirrors its mortality rate with a 5-year survival lower than 5% [1]; at diagnosis, less than 20% of patients are candidates for surgery with curative intent [2]. Standard treatments for advanced disease include radiotherapy and/or chemotherapy regimens. Radiotherapy has been shown to have some utility for regional confined cancers, but is often too toxic for tissues surrounding the neoplasia. Widely used chemotherapeutic regimes include 5-fluorouracil (5-FU) and gemcitabine, a nucleoside analogue of cytidine (2′,2′-difluorodeoxycytidine; dFdC) (GEM) [3]. However, even GEM, which is now considered the gold standard, has a response rate of less than 20%, although it does provide an improvement in the quality of life [4].

* Corresponding author. Dipartimento di Scienze Morfologico-Biomediche, Sezione Chimica Biologica, Università degli Studi di Verona, Strada Le Grazie, 8, 37134 Verona, Italy. Tel.: +39 045 8027169; fax: +39 045 8027170.
E-mail address: marta.palmieri@univr.it (M. Palmieri).
[1] Present address: Medical Oncology, Ospedale di Arzignano, ULSS n. 5 Ovest Vicentino, Vicenza, Italy.
[2] Authors share the last authorship.

0167-4889/$ - see front matter © 2007 Elsevier B.V. All rights reserved.
doi:10.1016/j.bbamcr.2007.05.002

Several mechanisms of resistance to GEM have been described, such as inefficient cellular uptake due to low expression of nucleoside transporters (NTs) [5], reduced levels of the activating enzyme deoxycytidine kinase (dCK) [6] and increased cytidine deaminase (CDD) [7] or cytoplasmic 5′ nucleotidase (5NT) activities, which lead to GEM inactivation [6–8] and loss of sensitivity of ribonucleotide reductase (RNR) to GEM inhibition [9]. p53, the guardian of genome integrity that typically induces the apoptotic response of cells to DNA damaging drugs, is also involved in the resistance to GEM [10]. Indeed, pancreatic cancer cells, which present a high rate of mutations of the *TP53* gene [11], have been shown to strongly increase GEM sensitivity after reintroduction of the wild type *TP53* gene *in vitro* and *in vivo* [12,13]. Recently, it has been reported that an increased expression of selenoprotein P, which suppress the intracellular free radicals, determines resistance to GEM, strongly suggesting that the oxidative stress could be a novel mechanism of GEM action [14].

Among multiple genetic and cytogenetic alterations that characterize human tumours, great emphasis was recently given to epigenetic events, such as DNA methylation or histone acetylation [15]. Alterations in histone acetyl transferase (HAT) or histone deacetylase (HDAC) activity occur in numerous cancers and have prompted the search for pharmacological agents capable of inhibiting these enzymes [16]. HDAC inhibitors seem to be specifically selective against tumour cells [17,18] and show a very low toxicity *in vivo* [19,20]. Trichostatin A (TSA) is one of the natural inhibitors of HDAC that promotes histone hyperacetylation and strongly induce apoptosis, by altering the expression of some apoptotic genes [21–25].

We have previously shown that TSA induces apoptosis and G2-phase cell cycle arrest in *TP53* mutated pancreatic cancer cell lines [23]. Moreover, we have reported that TSA enhances the response of a panel of five chemotherapeutic drugs on ten pancreatic adenocarcinoma cell lines and that it is the best partner for the gold standard GEM [26].

Here, we have characterized the mechanisms responsible for pancreatic cancer cell growth inhibition by TSA and GEM, both *in vitro* and *in vivo,* and analyzed whether TSA affects the molecular events implicated in GEM resistance. Our results demonstrate that TSA synergistically increases GEM-induced cell growth inhibition of four pancreatic adenocarcinoma cell lines, all with mutations in the *TP53* gene [11]. This synergistic effect depends on apoptosis, but not cell cycle arrest induction, and is strictly related to (i) the activation of the oxidative stress by GEM; (ii) the repression of the 5′-nucleotidase *UMPH* type II gene by TSA; (iii) the enhancement of the proapoptotic *BIM* expression by TSA and GEM. We also report that the sensitivity to GEM in 10 pancreatic adenocarcinoma cell lines is related to the intrinsic ROS stress. Finally, we show that the combined treatment with TSA and GEM significantly inhibits subcutaneous growth of human pancreatic adenocarcinoma in nude mice, whereas single treatments have no effect.

2. Materials and methods

2.1. Chemicals

Trichostatin A (TSA) was obtained from Sigma-Aldrich Company Ltd., solubilised in DMSO and stored at −80 °C until use. Gemcitabine (GEM; Gemzar, Lilly) and *N*-acetyl-L-cysteine (NAC) (Sigma) were freshly prepared in sterile water.

2.2. Cell culture

Ten human pancreatic cancer cell lines were used, comprising seven cell lines derived from primary cancer (MiaPaca2, PaCa3, PaCa44, PANC1, PT45P1, PSN1, and PC) and three from metastatic cancers (HPAF II, CFPAC1, and T3M4) (see [11] for genetic characterization and primary tissue source). All cell lines were grown in RPMI 1640 supplemented with 20 mM glutamine, 10% FBS and 50 μg/ml gentamicin sulfate (BioWhittaker, Italy) and were incubated at 37 °C with 5% CO_2.

2.3. Cell proliferation assay

Cells were plated in 96-well cell culture plates (4×10^3 cells/well) and were treated with TSA and/or GEM at the indicated concentrations. Treated cells were maintained at 37 °C in 5% CO_2 for times indicated in the legends to the figures, then stained with Crystal Violet (Sigma). The dye was solubilised in 1% SDS in PBS and measured photometrically ($A_{595\ nm}$) to determine cell viability. Three independent experiments were performed for each assay condition.

2.4. Drug combination studies

The combination index (CI) was calculated by the Chou–Talalay equation, which takes into account both the potency (D_m or IC_{50}) and the shape of the dose–effect curve [27,28], taking advantage of the CalcuSyn software (Biosoft, Cambridge, UK). The general equation for the classic isobologram (CI=1) is given by $CI=(D)_1/(D_x)_1+(D)_2/(D_x)_2+[(D_x)_1\cdot(D_x)_2]/[(D)_1+(D)_2]$, where $(D_x)_1$ and $(D_x)_2$ in the denominators are the doses (or concentrations) for D_1 (drug 1) and D_2 (drug 2) alone that gives x% inhibition, whereas $(D)_1$ and $(D)_2$ in the numerators are the doses of drug 1 and drug 2 in combination that also inhibited x% (i.e., isoeffective). CI<1, CI=1, or CI>1 generally indicated synergistic, additive, or antagonistic effect, respectively. However, we decided to use a cut off for the CI of 0.8, and identified a synergistic effect when CIs were smaller than 0.8, an antagonistic effect when they were greater than 1.2, and an additive effect when they were between 0.8 and 1.2. The linear correlation coefficient (r) of the median–effect plot is considered the first line of statistics to measure the conformity of the data with the mass–action law principle when the experimental measurement is assumed to be accurate. A r value equal to 1 indicates perfect conformity. A poor r value may be the result of biological variability or experimental deviations. For tissue culture systems a minimum r value of 0.90 should be obtained in order to consider the experiment valid. Throughout all the experiments we obtained a mean of $r=0.95\pm0.01$. Dose reduction index (DRI) represents the measure of how much the dose of each drug in a synergistic combination may be reduced at a given effect level compared with the doses of each drug alone. Treatment interaction effects between TSA and GEM were assessed at a concentration ratio 1:1. CI/fractional effect curves represent the CI versus the fraction of cells affected/killed by TSA and GEM in combination. The fractional effect is the % of growth inhibition corresponding to a given combination of the two drugs.

2.5. Cell cycle analysis

Cell cycle distribution was analyzed using propidium iodide (PI)-stained cells. Briefly, 10^6 cells were washed with PBS, incubated with 0.1% sodium citrate dihydrate, 0.1% Triton X-100, 200 μg/ml RNase A, 50 μg/ml propidium iodide (Roche Molecular Biochemicals) and analyzed using a flow cytometer (Becton Dickinson). The percentage of cells in the different stages of the cell cycle was determined using the ModFitLT software program.

2.6. Apoptosis

The percentage of apoptotic cells was evaluated by staining 2×10^5 cells with annexin V-FITC (Bender Med System, Vienna, Austria) and 5 mg/ml propidium iodide in binding buffer [10 mM HEPES/NaOH (pH 7.4), 140 mM NaOH, and 2.5 mM $CaCl_2$] for 10 min at room temperature in the dark. The samples were analyzed by flow cytometry (FACScalibur, Becton-Dickinson) within 1 h to determine the percentage of cells displaying annexin V^+/propidium iodide-(early apoptosis) or annexin V^+/propidium $iodide^+$ staining (late apoptosis). Three independent experiments were performed for each assay condition.

Caspase-3 activity was assayed as previously reported [23]. Briefly, after treatment with TSA, cells were washed twice with ice-cold PBS and lysed by freeze and thawing in caspase buffer (100 mM HEPES, 200 mM NaCl, 1 mM EDTA, 20 mM CHAPS, 10% sucrose). Hundred μg of total protein extract were incubated with 10 μg of the fluorogenic peptide substrate Ac-DEVD-AFC (PharMingen, San Diego, CA) 10 min at 30 °C and the release of 7-amino-4-methylcoumarin was determined fluorometrically using an excitation wavelength of 380 nm and an emission wavelength of 460 nm. Morphological changes of the cells were analyzed by staining with H&E. Cells treated with TSA and/or GEM presented features typical of apoptotic cells (data not shown).

2.7. Analysis of mitochondrial membrane potential (ΔΨm)

2×10^5 cells were stained with 40 nM 3,3-dihexyloxacarbocyanine (Molecular Probes) at 37 °C for 20 min, washed twice in PBS and then analyzed by flow cytometry. The percentage of cells exhibiting a decreased level of 3,3-dihexyloxacarbocyanine uptake that reflects loss of ΔΨm, was determined by flow cytometry.

2.8. Measurement of reactive oxygen species (ROS) production

The non-fluorescent 2′,7′-dichlorofluorescin (DCF) probe, which becomes highly fluorescent on reaction with ROS, was used to evaluate cellular ROS production [29]. Briefly, 2×10^5 cells were incubated with 10 μM DCF (Sigma) at 37 °C for 15 min and then analyzed by flow cytometry.

2.9. Small interfering RNA

Cells were plated in 96-well for proliferation assays (4×10^3 cells/well) or into 60 mm cell culture plates at 2.5×10^5 cells/plate for RNA extraction. After 24 h, growth medium was removed and fresh serum/antibiotics free medium was added. Cells (at ~30% confluency) were transfected with siRNA at a final concentration of 100 nM using jetSI-ENDO-Fluo cationic transfection reagent (Polyplus transfection, TEMA Ricerche, Italy) according to the manufacturer's transfection protocol. Silencing was performed by SMARTpool siRNAs (*BIM*: human *BCL2L11*, NM_006538; *UMPH* type II: human *NT5C*, NM_014595) purchased from Dharmacon (Tema Ricerche, Italy). A negative control designed to minimize targeting to any known human genes (siCONTROL Non-targeting siRNA pool, Dharmacon) was transfected to validate transfection results. Twenty-four hours after transfection TSA and/or GEM were added and cells were further incubated for 24 h before analysis. Transfection efficiency was assessed by cytofluorimetric analysis and ranged between 88 and 96%.

2.10. Immunoblot analysis

Protein extracts from 10^6 cells, untreated or treated with TSA, and from tumour mass, removed from both control and treated animal groups, were prepared in acid buffer (0.2 M Tris, 0.2 M HCl, 1 mM phenylmethylsulfonyl fluoride, 1% β-mercaptoethanol, 1× protease inhibitor cocktail) by freeze and thawing, and the lysate was clarified by centrifugation. Five μg of protein extracts were electrophoresed and blotted onto PVDF membranes (Millipore, Bedford, MA). Membranes were probed with anti-acetyl-Histone H4 polyclonal Ab (Upstate Biotechnology) or anti-human α-Tubulin mAb (Oncogene). Horseradish peroxidase conjugated anti-mouse IgG (Upstate Biotechnology) was used to detect specific proteins. Immunodetection was carried out using the chemiluminescent substrates (Pierce) and recorded by using a HyperfilmECL (Amersham Pharmacia Biotech).

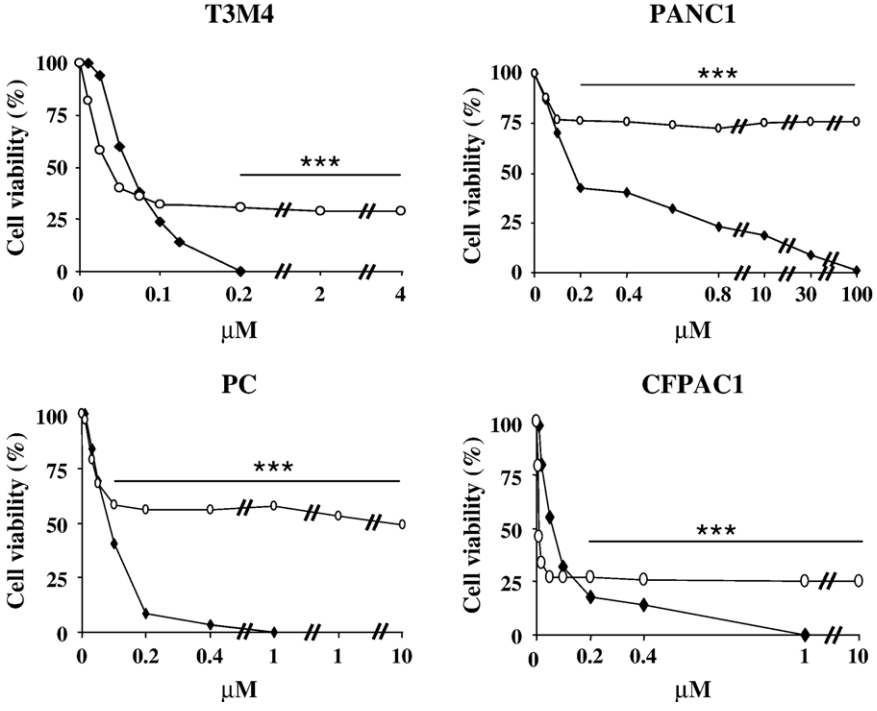

Fig. 1. Effect of TSA (♦) or GEM (○) treatment on growth of four pancreatic adenocarcinoma cell lines. Cells were seeded in 96-well plates and incubated overnight. TSA or GEM were added at the indicated concentrations and cells were further incubated for 48 h. Values are the means of triplicate wells from three independent experiments for each drug concentration. Cell proliferation was determined using the crystal violet colorimetric assay. ***$p<0.001$.

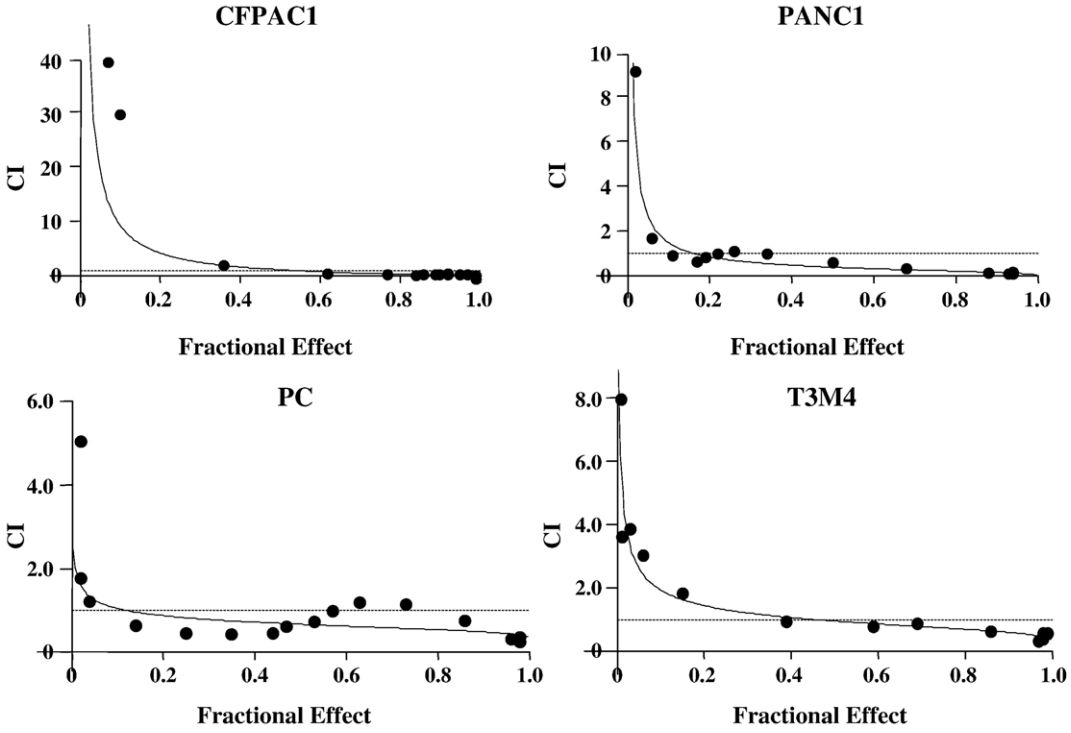

Fig. 2. CI /fractional effect curves for CFPAC, PANC1, PC, and T3M4 cells. A 1:1 molar ratio of TSA and GEM have been evaluated as described in Materials and methods. The figure shows the fractional effects vs. the different CIs. The fractional effect is the % of growth inhibition given by each combination of the two drugs. This value is represented on the *X* axis of the curve. CI values obtained by the same combinations are reported on the *Y* axis. When CI is below 0.8 a synergistic condition is recorded; with CI below 0.5 and between 0.8 and 1.0 a strong synergism or additivity, respectively, is found. The statistical significance of each point was evaluated with ANOVA and the derived *p* values were always less than 0.01.

2.11. RNA extraction, RT-PCR, and image analysis

Total cellular RNA was prepared from 5×10^6 cells and reverse transcribed as previously described [23]. The thermal cycler protocols and specific primers are the followings: *BIM* 5′-TGATATCAATGCATTCTCCACACCAGGCGGAC-3′ and 5′-AGAATTCATGGCAAAGCAACCTTCTGATGTAAG-3′, 94 °C (30 s), 56 °C (30 s), 72 °C (30 s), 30 cycles; *UMPH* type II 5′-ATGAACGACCTACCG-GACAC-3′ and 5′-CGGTAGCACAGCGCTTAACG-3′, 94 °C (30 s), 58 °C (30 s), 72 °C (1 min), 30 cycles; *β-ACTIN* 5′-ACCAACTGGGACGACATGGA-GAA-3′ and 5′-GTGGTGGTGAAGCTGTAGCC-3′, 94 °C (1 min), 55 °C (1 min), 72 °C (1 min), 25 cycles. PCR products were separated by electrophoresis and the bands were photographed and scanned as digital peaks. The areas of the peaks were calculated in arbitrary units using the public domain NIH Image program (developed at the U.S. National Institutes of Health and available on the Internet at http://rsb.info.nih.gov/nih-image/). *β-ACTIN* was used as an internal standard to evaluate the relative expression levels of target genes.

Table 1
Dose Reduction Index (DRI)[a] and Combination Index (CI)[b] values of TSA/GEM combination on different pancreas cancer cell lines

Cell lines	Molar ratio 1:1						
	TSA/GEM						
	ED_{50} (nM)	ED_{75} (nM)	CI_{50} (±SEM)	CI_{75} (±SEM)	DRI_{50} (±SEM)	DRI_{75} (±SEM)	*r*
T3m4	21.9	37.2	0.8 (0.17)	0.7 (0.0685)	1.5 (0.12) 5.4 (0.55)	1.7 (0.1) 9.8 (1.12)	0.99
PANCI	79.8	193.1	0.4 (0.05)	0.2 (0.025)	3.3 (0.38) 13.1 (1.12)	4.7 (0.36) 35 (2.78)	0.98
PC	42.7	103.8	0.6 (0.042)	0.5 (0.08)	3.1 (0.189) 3.8 (0.25)	3.1 (0.26) 5.5 (0.59)	0.97
CFPAC1	11.9	32	1.0 (0.123)	0.4 (0.036)	8.9 (0.96) 1.1 (0.25)	8.6 (0.96) 3.1 (0.42)	0.95

(DRI_{50}) and IC_{75} (DRI_{75}) in combination setting compared with each drug alone. 1:1 molar ratio of the two agents was used. Combination index (CI) values of <1, 1, and >1 indicate synergy, additivity, and antagonism, respectively.

[a] DRI values (mean±Standard Error of the Mean (SEM) from at least three separate experiments performed in quadruplicates) represent the order of magnitude (fold) of dose reduction obtained for IC_{50}.

[b] CI values (mean±Standard Error of the Mean (SEM) from at least three separate experiments performed in quadruplicates) represent the assessment of synergy induced by drug interaction when 50% (CI_{50}) or 75% (CI_{75}) growth inhibition is recorded.

Table 2
Treatments of human pancreatic tumours in nude mice with TSA (0.25 mg/kg) and GEM (2.5 mg/kg) biweekly for 4 weeks

Treatment	Mean tumour weight g (±SEM)	Mean tumour weight g % (±SEM)	Mean body weight g (±SEM)	No. of dead mice/ No. of total mice
Control	5.74±0.8	100±29	24.4±1.0	0/5
TSA (0.25 mg/kg)	6.34±0.5	110±17	24.4±0.7	0/5
GEM (2.5 mg/kg)	5.98±0.7	104±28	27.1±1.7	0/5
TSA+GEM	2.98±0.7*	52±26 *	24.9±1.4	0/5

*$p<0.05$.

2.12. In vivo studies

To examine the *in vivo* cells growth inhibition, T3M4 human pancreatic cancer cells (5×10^6 cells for each mice) were s.c. injected into female nude mice (4 weeks of age, Charles River Laboratories, Italy). One week after cell inoculation, 5 randomized animals for each experimental group received vehicle control (DMSO) or TSA or GEM or TSA plus GEM at doses indicated in the tables by i.p. injection twice weekly for 4 weeks. Doses were chosen in initial dose-ranging evaluations, on the basis of the absence of any measurable toxicity. None of the treatments produced any toxicity as indicated by lack of change in body weight (Table 2) and none of the animals developed ulcerating tumours. No deaths were observed among any of the considered groups of mice. At the end of the treatments, mice were sacrificed and subcutaneous tumours were carefully dissected free of the surrounding normal tissue and weighed. Weekly, tumour volumes and body mass were recorded for each animal. Animals were sacrificed at the end of the 4-week study period. Palpable tumours were resected, weighted and immediately snap-frozen in liquid nitrogen. The animal studies were approved by the Verona University Review Board.

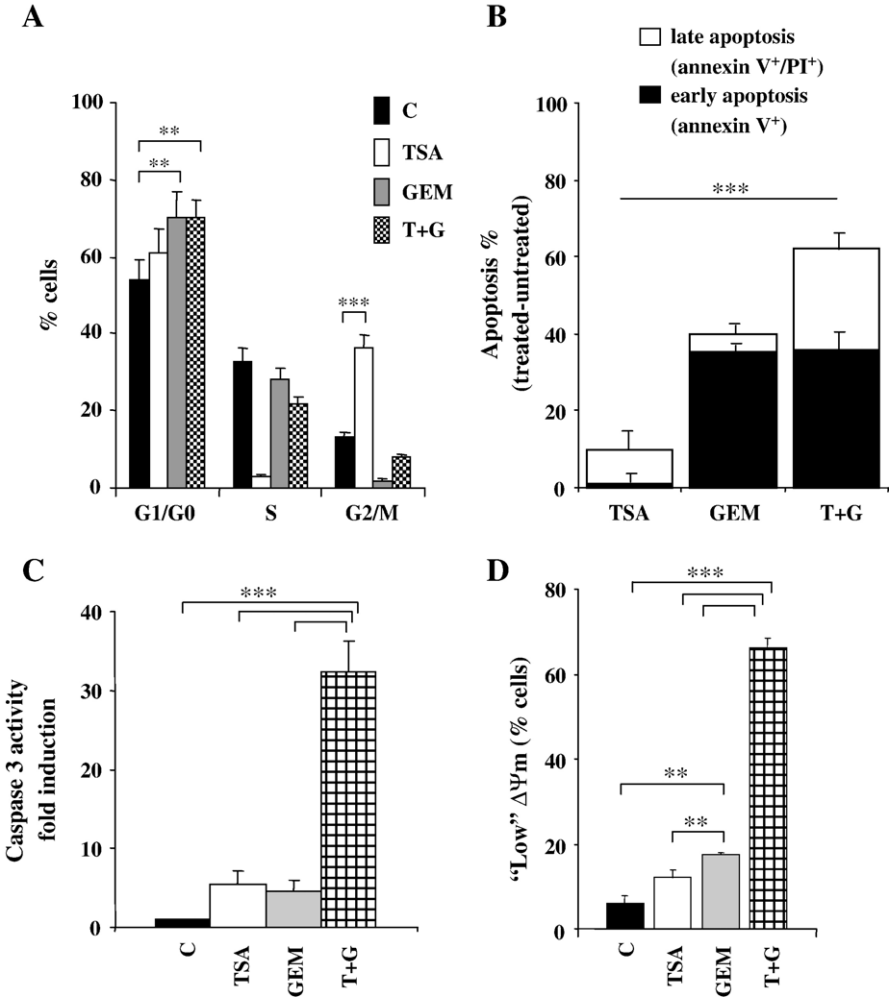

Fig. 3. (A) Cell cycle distribution after TSA and/or GEM treatment. T3M4 cells were treated with 0.2 μM TSA and/or 2 μM GEM for 24 h. Cell cycle distribution was analyzed by a flow cytometer after DNA staining with propidium iodide. (B) Induction of apoptosis by TSA and/or GEM. T3M4 cells were treated as in (A) and analyzed by flow cytometry to determine the percentage of cells displaying annexin V^+(early apoptosis) or annexin V^+/ propidium $iodide^+$ staining (late apoptosis). The percentage apoptosis was calculated by subtracting the untreated control values from the treated values. (C) Induction of caspase 3 activity by TSA and/or GEM. T3M4 cells were treated as in (A) and caspase 3 activity was assessed. (D) Effect of TSA and/or GEM on mitochondrial membrane potential ($\Delta\Psi$m). T3M4 cells were treated with 0.2 μM TSA and/or 2 μM GEM for 48 h and the percentage of cells exhibiting reduced $\Delta\Psi$m was determined by flow cytometry using 3,3-dihexyloxacarbocyanine staining. Values are the means±SEM of three independent experiments. **$p<0.01$; ***$p<0.001$.

2.13. Statistical analysis

ANOVA (post hoc Bonferroni) analysis and graphical presentations were performed by GraphPad Prism version 5. p values less than 0.05, 0.01 or 0.001 were indicated as *, ** or ***, respectively. Data in Fig. 6C were analyzed by paired t test.

3. Results

3.1. TSA and GEM synergistically inhibit proliferation of human pancreatic adenocarcinoma cell lines in vitro

Dose-dependent curves of cell viability of pancreatic adenocarcinoma cell lines treated with TSA or GEM are shown in Fig. 1. GEM engendered a plateau of survival ranging from 75% (PANC1) to 25% (T3M4), while TSA was generally more active than GEM and did not show a saturating effect. To test the effect of a combined treatment with TSA and GEM on cell growth, we performed drug combination studies using a dedicated software (Calcusyn, see Materials and methods) for the elaboration of the results. CI/fractional effect curves showing the CIs versus the fraction of cells affected/killed by TSA and GEM in combination, for the different cell lines, are illustrated in Fig. 2. The fractional effect is the % of growth inhibition given by each combination of the two drugs. This value was represented on the X axis of the curve, while on the Y axis CI given by the same combination was reported. When CI is below 0.8 a synergistic condition was recorded; with CI

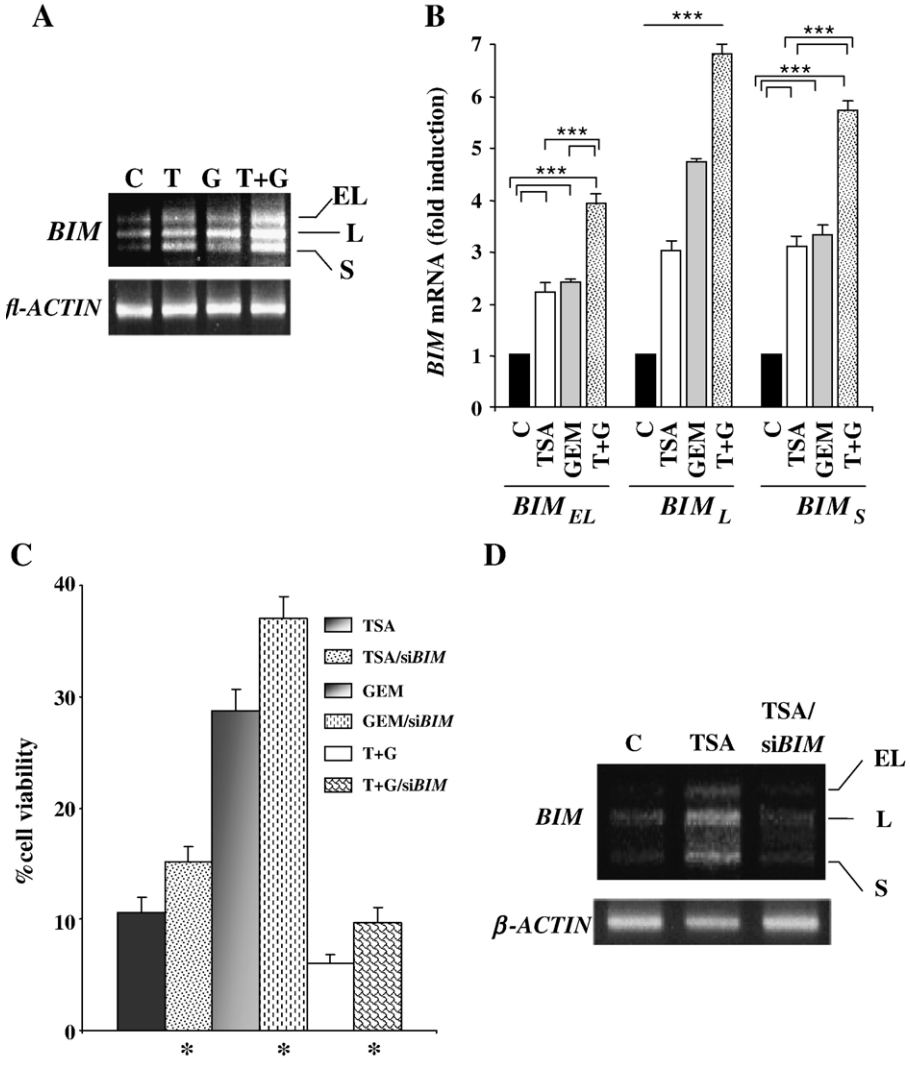

Fig. 4. RT-PCR analysis of the *BIM* mRNA after treatment with TSA and/or GEM and RNA interference assay. (A) Electrophoretic analysis. Samples were obtained from T3M4 cells treated with 0.2 μM TSA and/or 2 μM GEM for 8 h. mRNAs of the three *BIM* isoforms (BIM_{EL}, BIM_L and BIM_S), derived from alternative splicing [31] are indicated. Primer sequences and PCR conditions are indicated in Materials and methods. A representative experiment is shown. (B) Densitometric analysis. The intensity of bands corresponding to *BIM* (EL, L, and S) relative to β-actin is shown. Values are the means ± SEM of three independent experiments. ***$p<0.001$. (C) siRNA. T3M4 cells were transfected with a *BIM* siRNA SMARTpool in serum/antibiotics free medium and 4 h after transfection complete medium was restored. TSA (0.2 μM) and/or GEM (2 μM) were added 24 h after transfection and cells were further incubated for 48 h. Percentage of cell survival was evaluated using the crystal violet colorimetric assay. Values are the means ± SEM of three independent experiments. *$p<0.05$. (D) RT-PCR analysis of the *BIM* mRNA expression after RNA interference. Transfections were carried out as described in Materials and methods. mRNAs of the three *BIM* isoforms (BIM_{EL}, BIM_L and BIM_S), derived from alternative splicing [31] are indicated. Primer sequences and PCR conditions are shown in Table 2. A representative experiment is shown.

below 0.5 and between 0.8 and 1.0 a strong synergism or additivity, respectively, was found.

In synergistic drug combination the CI_{50s} (the combination index calculated for 50% cell survival by isobologram analysis) were, at 1:1 molar ratio of both drugs, respectively, 0.8, 0.4, 0.6 and 1.0 for T3M4, PANC1, PC and CFPAC1 cells (Table 1). In the same experimental conditions the CI_{75s} (the combination index calculated for 75% cell survival by isobologram analysis) were, respectively, 0.7, 0.2, 0.5 and 0.4 for T3M4, PANC1, PC and CFPAC1 cells (Table 1). The analysis of CIs revealed that TSA and GEM combinations were globally synergistic (CIs<0.8) in all cell lines but in CFPAC1 where a clear synergistic effect was observed only when TSA was combined with GEM at concentrations able to induce 75% growth inhibition (CI_{75}=0.4) (Fig. 2, Table 1).

Notably, in all cell lines, a 1.5- up to 13.1-fold reduction in the IC_{50} of both TSA and GEM (DRI_{50}) was observed in the combination setting compared with the concentrations of the drugs used alone (Table 2). Interestingly, the values of *r* factor were always between 0.95 and 0.99 suggesting that the data were statistically significant (Table 1).

3.2. TSA enhances apoptosis but not cell cycle arrest induced by GEM

The analyses of flow cytometry with annexin V-FITC and propidium iodide staining and of caspase 3 activity show that either TSA or GEM gave rise to an apoptotic effect, which was strongly increased in the presence of both drugs (Fig. 3B and Fig. 3C). The potentiation of apoptosis occurred on both late and early phase of programmed cell death. The combined treatment, on the contrary, did not further increase cell cycle arrest determined by single drugs (Fig. 3A). Fig. 3D shows that the percentage of cells presenting a reduced mitochondrial membrane potential ($\Delta\Psi$m) was strongly increased by TSA and GEM combination as compared to single drugs, suggesting the involvement of the mitochondrial pathway in the induction of apoptosis by the drug combination.

3.3. Bim has a role in growth inhibition by TSA and GEM

The Bcl-2 family of proteins plays a critical role in regulating programmed cell death involving the mitochondrial pathway [30]. We show here that the combined treatment of T3M4 cells with TSA and GEM combination significantly increased mRNA expression of the three *BIM* isoforms (BIM_{EL}, BIM_L and BIM_S), derived from alternative splicing [31], compared to single treatments (Fig. 4A and Fig. 4B).

To verify a direct role of Bim in TSA- and GEM-induced growth inhibition, we performed proliferation assays in T3M4 cell line using RNA interference (RNAi) technology to knock down endogenous *BIM*. The results shown in Fig. 4C demonstrated that silencing of *BIM* (see Fig. 4D) significantly contributed to protect cells ($p<0.05$) from growth inhibition by TSA and/or GEM, indicating that Bim has a role in cell death by both single and combined drug treatments.

3.4. GEM increases oxidative cellular stress

The induction of ROS has been described to increase mitochondrial membrane permeability, thus promoting apoptosis [32]. We analyzed ROS level in T3M4 cells after TSA and/or GEM treatment. Fig. 5A shows that ROS levels were increased of approximately 2-fold by GEM, while they were not affected by TSA and not further increased by the combined treatment. Depletion of ROS by the free radical scavenger NAC was able to significantly decrease the level of cell growth inhibition by GEM (Fig. 5B), indicating that ROS production plays a role in GEM induced cytotoxic effect. Furthermore, we observed that treatment of cells with TSA and H_2O_2 significantly increased growth inhibition compared to single agent (data not shown). Taken together these results indicate that ROS production is involved in the induction of cell growth inhibition by GEM and may contribute to the synergistic growth inhibition by TSA and GEM combined treatment.

To further confirm a potential role of the oxidative stress in the sensitivity of pancreatic adenocarcinoma cells to GEM, we

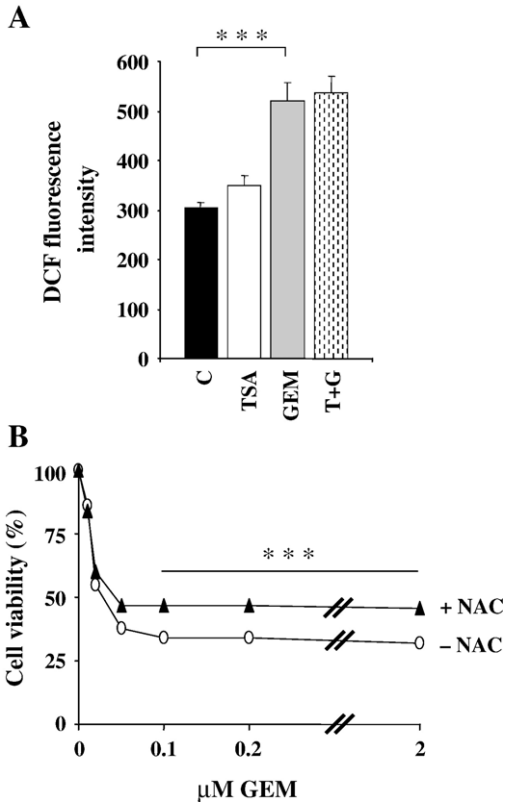

Fig. 5. (A) Effect of TSA and/or GEM on ROS production. T3M4 cells were treated with 0.2 μM TSA and/or 2 μM GEM for 16 h. The 2′,7′-dichlorofluorescin (DCF) fluorescence intensity, corresponding to the level of ROS production, was measured by flow cytometry as described in Materials and methods. Values are the means±SEM of three independent experiments. ***$p<0.001$. (B) Effect of NAC on cell growth inhibition by GEM. T3M4 cells were treated with increasing concentrations of GEM in the absence or presence of NAC (1 mM) for 48 h. Values are the means of triplicate wells from three independent experiments for each drug concentration. ***$p<0.001$. Cell proliferation was determined using the crystal violet colorimetric assay. Treatment with 1 mM NAC alone did not affect cell growth.

compared the IC_{50} values of 10 pancreatic adenocarcinoma cell lines with their respective basal oxidative stress. Fig. 6 shows that the cell lines with a lower basal level of ROS were more resistant to GEM (Fig. 6A) compared to the less resistant cell lines (Fig. 6B).

3.5. 5′-nucleotidase UMPH type II has a role in growth inhibition by GEM

To assess whether TSA affects critical molecular mechanisms generally associated with GEM resistance, we analyzed by RT-PCR the expression levels of the genes for nucleoside transporters (*CNT1*, *CNT2*, *CNT3*, *ENT1*, and *ENT2*), deoxycytidine kinase (*dCK*), 5′-nucleotidases (*cN-I*, *cN-II*, and *UMPH* type I and II) I, cytidine deaminase (*CDD*), and the two ribonucleotide reductase subunits (*RRM1* and *RRM2*). The analysis of mRNAs for those genes showed that the level of *UMPH* type II mRNA was down-regulated after 8 h TSA treatment (Fig. 7A and Fig. 7B), whereas the levels of the other mRNAs were not affected (not shown).

To assess the role of 5′-nucleotidase UMPH type II on the sensitization by TSA of GEM-induced cell growth inhibition,

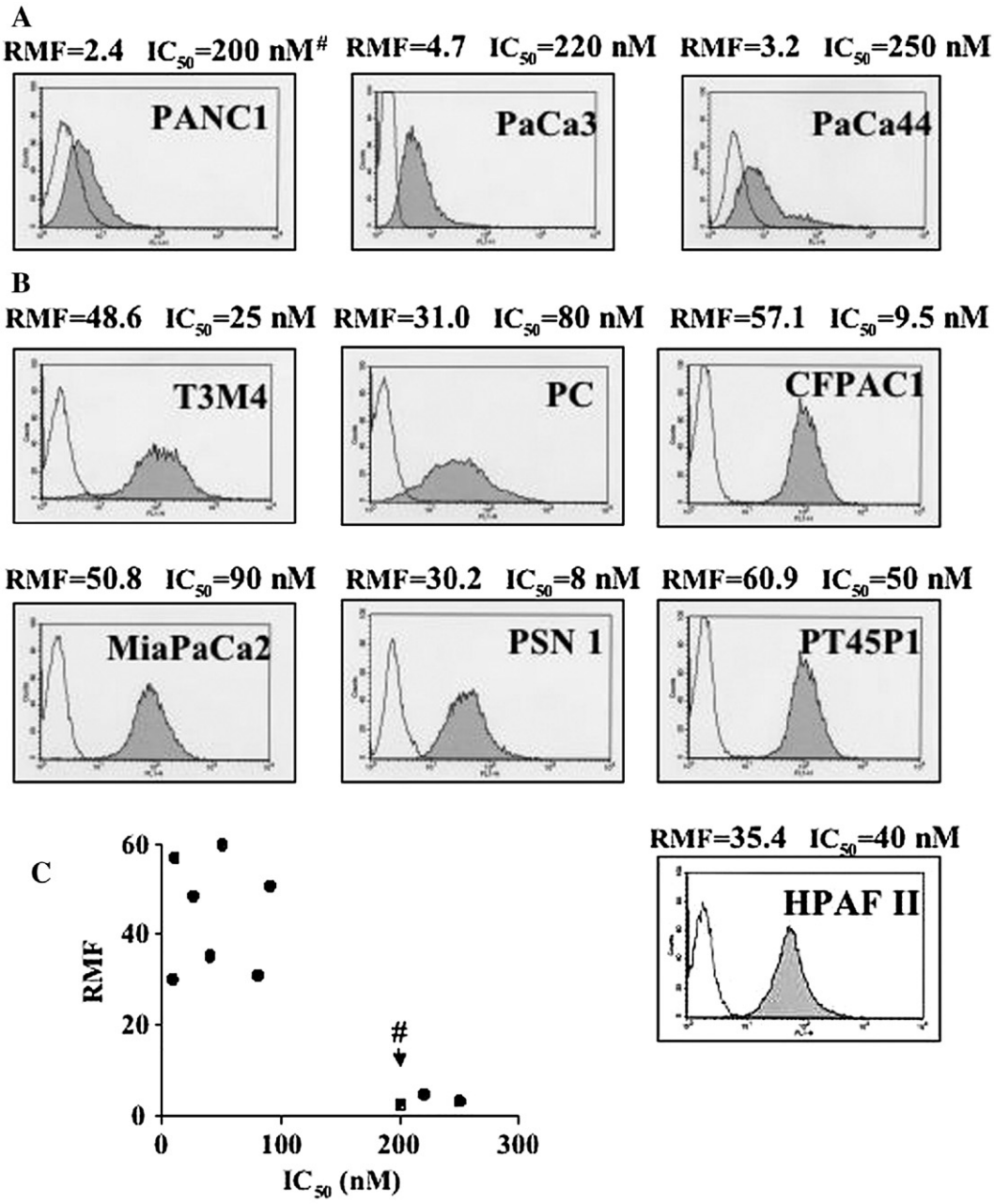

Fig. 6. Comparison between intrinsic ROS production and GEM sensitivity in ten pancreatic adenocarcinoma cell lines. (A) Cell lines showing the lowest values of the relative mean fluorescence (RMF) and the highest IC_{50} values of GEM. (B) Cell lines showing the highest values of the relative mean fluorescence (RMF) and the lowest IC_{50} values of GEM. RMF is the ratio between fluorescence intensity of cells treated and untreated (autofluorescence) with DCF. The 2′,7′-dichlorofluorescin (DCF) fluorescence intensity corresponding to the cellular ROS level was measured by flow cytometry as described in Materials and methods. #The lowest GEM concentration determining maximal PANC1 cell line growth inhibition. (C) Diagram showing RMF versus IC_{50}. #The lowest GEM concentration determining maximal PANC1 cell line growth inhibition. Paired *t* test of IC_{50} and RMF values between cell lines shown in A and B: $p<0.001$.

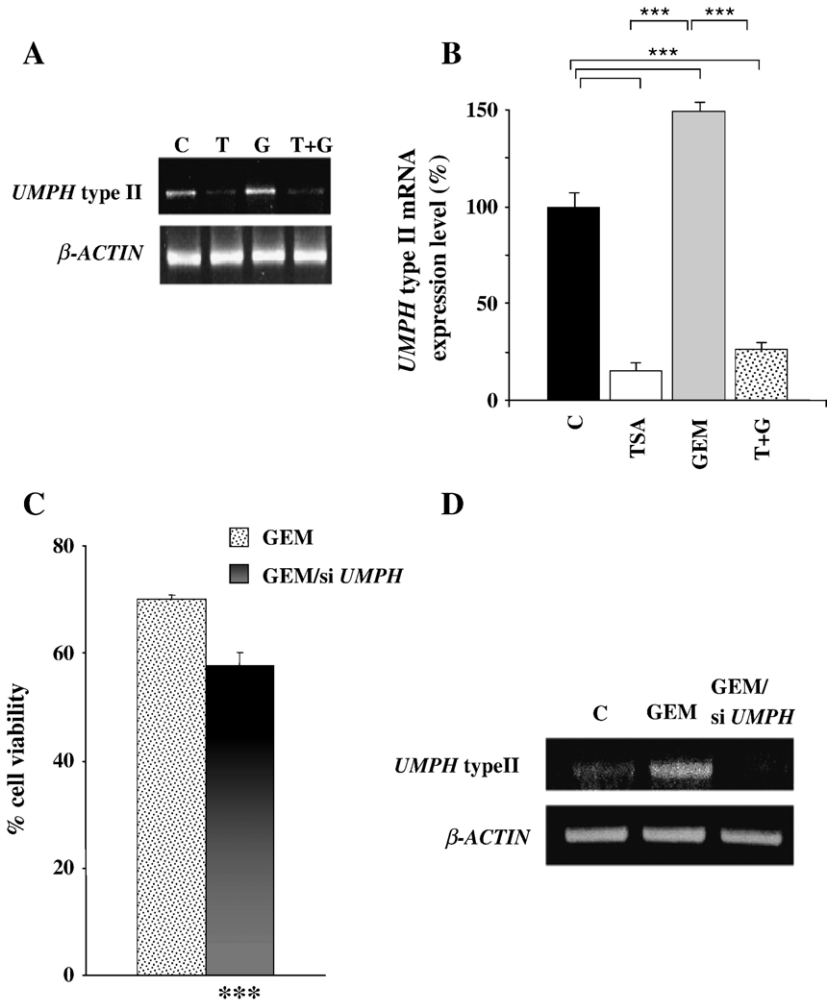

Fig. 7. RT-PCR analysis of the *UMPH* type II mRNA expression after treatment with TSA and/or GEM and RNA interference assay. (A) Electrophoretic analysis. Samples were obtained from T3M4 cells treated with 0.2 μM TSA and/or 2 μM GEM for 8 h. Primer sequences and PCR conditions are indicated in Materials and methods. A representative experiment is shown. (B) Densitometric analysis. The intensity of *UMPH* type II band relative to β-actin is shown. Values are the means± SEM of three independent experiments. ***$p<0.001$. (C) siRNA. T3M4 cells were transfected with a specific siRNA SMARTpool for *UMPH* type II in serum/antibiotics free medium and 4 h after transfection complete medium was restored. GEM (2 μM) was added 24 h after transfection and cells further incubated for 24 h. Percentage of cell survival was evaluated using the crystal violet colorimetric assay. ***$p<0.001$. (D) RT-PCR analysis of the *UMPH* type II mRNA expression after RNA interference. Transfections were carried out as described in Materials and methods. Primer sequences and PCR conditions are indicated in Materials and methods. A representative experiment is shown.

we carried out proliferation assays in T3M4 cells using siRNA technology. Following *UMPH* type II gene silencing, cell growth inhibition by GEM was significantly increased ($p<0.001$) (Fig. 7C and Fig. 7D), strongly suggesting a role of UMPH type II for the synergistic effect by TSA and GEM.

3.6. TSA and GEM synergistically inhibit growth of human pancreatic adenocarcinoma cells in vivo

The effect of TSA and/or GEM on growth inhibition of pancreatic cancer cells *in vivo* was examined on subcutaneous xenografts of T3M4 cells in nude mice. As shown in Table 2, TSA or GEM did not cause any significant suppression of tumour growth, while the combination of the two drugs determined a reduction in the mean tumour weight of about 50% compared to control or single drug treatments (Table 2). The same result was obtained using higher doses of drugs, i.e. 1 mg/kg of TSA and/or 25 mg/kg of GEM (data not shown). To test whether TSA effectively inhibited histone deacetylase (HDAC) enzymes in the tumour mass, we examined the levels of H4 histone acetylation in the dissected tumours from mice untreated or treated with TSA. Fig. 8 shows that TSA treatment determined only a 3-fold increase of H4 acetylation levels *in vivo*, at both concentrations tested, compared to the 18-fold increase *in vitro*. On the other hand, GEM alone did not induce changes in histone acetylation (data not shown).

4. Discussion

In this study, we have evaluated the *in vitro* and *in vivo* effects of TSA and GEM on human pancreatic adenocarcinoma cell growth. We report that treatment with increasing concentrations

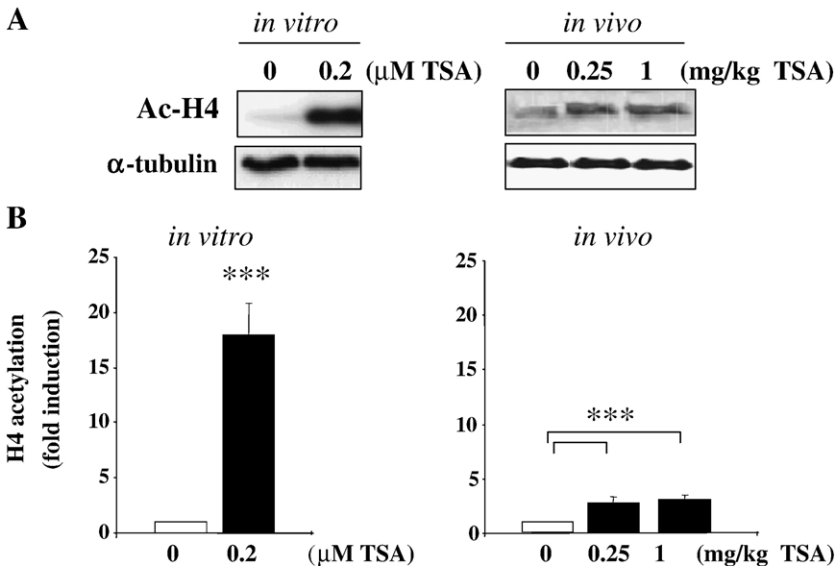

Fig. 8. Western blot analysis of acetylated histone H4. (A) T3M4 cells were treated with 0.2 μM TSA for 4 h *in vitro*. Nude mice with subcutaneous xenografts of T3M4 cells were injected with 0.25 mg/kg or 1 mg/kg TSA biweekly for 4 weeks and sacrificed 4 h after the last TSA injection. Protein extracts were obtained as described in Materials and methods. (B) The fold induction of histone H4 acetylation was measured by densitometric analysis. Mean values±SEM are reported. ***$p<0.001$.

of GEM of different pancreatic adenocarcinoma cell lines, all having mutations in the p53 gene, determines a plateau of survival ranging from 75% to 25% compared to untreated cells. This result suggests a mechanism of drug resistance, which is not observed with TSA that induces a complete growth inhibition of cells.

Resistance to the cytotoxic effect of GEM can be related to multiple mechanisms including alteration of apoptosis regulating genes [10], alterations in the transport and cellular turnover of the drug as well as altered expression or sensitivity of enzyme targets [5–9,33]. p53 mutations, which are very frequent in pancreatic cancer [11], reduce gemcitabine-induced apoptosis [10]. We [23] and others [21] have published that TSA induces apoptosis in p53-negative cancer cells, suggesting that p53 plays a minor role in the cellular effects of TSA. Moreover, our earlier studies on mitochondrial related apoptotic genes demonstrate that the proapoptotic gene *BIM* is significantly upregulated by TSA, whereas the antiapoptotic *BCL-XL* and *BCL-W* genes are downregulated [24]. Furthermore, it has been reported that an increased ratio of expression levels of the proapoptotic genes versus antiapoptotic *BCL-2* sensitizes pancreatic cancer cells to GEM treatment [34–37]. Here, we demonstrate that GEM further increases TSA induced *BIM* mRNA and that *BIM* silencing significantly reduces growth inhibition of pancreatic adenocarcinoma cell lines by TSA and/or GEM, strongly suggesting the involvement of Bim in the cell death induction by the two drugs. These data are in agreement with the results of Zhao et al., who have reported that Bim is a key mediator of the apoptotic process induced by TSA in p53-null HCT116 stably expressing E2F1 [25].

The generation of free radicals is generally related to the loss of mitochondrial inner membrane potential and is considered one of the cytotoxic activities of GEM [14], although the precise mechanism responsible for such stress remains to be defined. In our study, we find that GEM induces an approximately 2-fold increase of intracellular free radicals and that 1 mM of the radical scavenger NAC is able to rescue, at least in part, the antiproliferative effect of GEM. Higher concentrations of NAC, which could further reduce cell growth inhibition by GEM, are toxic to pancreatic adenocarcinoma cells, as already reported in other systems [38]. It is known that the increase in ROS stress can induce various biological responses, including cellular proliferation, apoptosis, and necrosis [32]. Cancer cells are known to be metabolically active and under increased oxidative stress, which makes them highly dependent on antioxidant enzymes to cope with the stress of ROS [32,39]. It has been demonstrated that further oxidative stress such as the exposure of cancer cells to ROS-generating anticancer agents exhausts the cellular antioxidant capacity and leads to apoptosis probably by pushing the ROS stress level beyond a threshold [32,39].

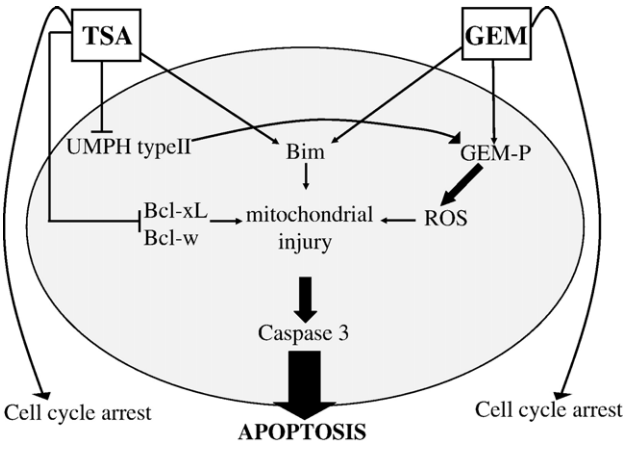

Fig. 9. Model of activation of the apoptotic cascade by the combined action of TSA and GEM in pancreatic adenocarcinoma cells.

Consistent with this observation, we have shown a positive correlation between intrinsic ROS stress and sensitivity to GEM in 10 pancreatic adenocarcinoma cell lines. Furthermore, we demonstrate that H_2O_2 significantly enhances cell growth inhibition by TSA (data not shown), suggesting that ROS production by GEM is an important element in the synergistic inhibition of pancreatic cancer cells by TSA and GEM.

The analysis of the regulation by TSA of critical molecular mechanisms generally associated with GEM resistance has shown that only the mRNA of the 5′-nucleotidase *UMPH* type II was regulated after TSA treatment. As UMPH type II is known to prevent the formation of the active forms of GEM [8], inhibition of UMPH type II by TSA may be another mechanism by which the two drugs synergistically inhibit pancreatic adenocarcinoma cell proliferation. Indeed, RNA interference experiments demonstrate that *UMPH* type II silencing sensitizes T3M4 cells to GEM. These data may support the idea that the development of new specific inhibitors of this enzyme could potentiate the antiproliferative effect of GEM.

Our *in vitro* results are summarised in the model shown in Fig. 9. Two recent reports have dealt with the effects of the combination of GEM with two HDAC inhibitors, 4-phenylbutirrate (4-PB) and suberoylanilide acid (SAHA), on the growth of pancreatic cancer cell lines *in vitro* [40,41]. These studies show that 4-PB and SAHA inhibit cell growth at concentrations much higher than those used for TSA in this paper, either alone or in combination with GEM. In addition, while 4-PB is shown to inhibit cellular export that may thus increase the sensitivity to GEM, SAHA is shown to exert proapoptotic effects by upregulating p21 and sequestering it in the cytoplasm. Neither study has analyzed the biochemical pathways shown here to play a role in cell growth inhibition by TSA/GEM. In addition, neither study reports *in vivo* experiments, which in our opinion strongly contribute to the suggestion that GEM in combination with HDAC inhibitors may represent a good candidate therapy for pancreatic cancer. Although we do not exclude the possibility that the molecular mechanisms described by Ammerpohl et al. and Arnold et al. [40,41] may also act in our system, we believe that the activation of the apoptotic cascade illustrated by the model of Fig. 9, which takes into account crucial aspects of TSA and GEM activity, may better explain the synergism between the two molecules.

In vivo experiments have shown that intraperitoneal injection of either TSA (0.25 mg/kg) or GEM (2.5 mg/kg) into nude mice that bear a subcutaneous mass of pancreatic adenocarcinoma cells cannot arrest tumour growth, while combined treatments can reduce to 50% the tumour mass. We have also observed that higher doses of GEM (25 mg/kg), comparable to that used in clinical trials [42,43], are not able to significantly inhibit pancreatic adenocarcinoma cell growth *in vivo* and do not further enhance growth inhibition obtained with the lower doses of TSA and GEM, when used in combination with higher doses of TSA (1 mg/kg). This result suggests that low doses of TSA may sensitize cells to overcome GEM resistance. It is noteworthy that all the *in vivo* treatments did not determine any apparent form of toxicity *in vivo*, as we did not observe mice deaths, body weight variations or other apparent toxicity-related features. This result may be ascribed to the fact that GEM is a well-tolerated chemotherapeutic agent [44] and that HDAC inhibitors seem to be specifically selective against tumour cells [17,18] and show a very low toxicity *in vivo* [19,20].

In conclusion, the present study describes the molecular mechanisms underlying the synergistic inhibition of pancreatic cancer cell growth *in vitro* by TSA and GEM. Moreover, the significant *in vivo* antitumour activity by TSA and GEM, together with the absence of toxicity, provide a rationale basis for the development of novel therapies in pancreatic cancer using the gold standard GEM in combination with an HDAC inhibitor.

References

[1] D. Li, K. Xie, R. Wolff, J.L. Abbruzzese, Pancreatic cancer, Lancet 363 (2004) 1049–1057.

[2] J.P. Neoptolemos, D. Cunningham, H. Friess, C. Bassi, D.D. Stocken, D.M. Tait, J.A. Dunn, C. Dervenis, F. Lacaine, H. Hickey, M.G. Raraty, P. Ghaneh, M.W. Buchler, Adjuvant therapy in pancreatic cancer: historical and current perspectives, Ann. Oncol. 14 (2003) 675–692.

[3] D.G. Haller, New perspectives in the management of pancreas cancer, Semin. Oncol. 30 (2003) 3–10.

[4] H.A. Burris III, M.J. Moore, J. Andersen, M.R. Green, M.L. Rothenberg, M.R. Modiano, M.C. Cripps, R.K. Portenoy, A.M. Storniolo, P. Tarassoff, R. Nelson, F.A. Dorr, C.D. Stephens, D.D. Von Hoff, Improvements in survival and clinical benefit with gemcitabine as first-line therapy for patients with advanced pancreas cancer: a randomized trial, J. Clin. Oncol. 15 (1997) 2403–2413.

[5] M.L. Clarke, J.R. Mackey, S.A. Baldwin, J.D. Young, C.E. Cass, The role of membrane transporters in cellular resistance to anticancer nucleoside drugs, Cancer Treat. Res. 112 (2002) 27–47.

[6] V.W. Ruiz van Haperen, G. Veerman, S. Eriksson, A.P. Stegmann, G.J. Peters, Induction of resistance to 2′,2′-difluorodeoxycytidine in the human ovarian cancer cell line A2780, Semin. Oncol. 22 (1995) 35–41.

[7] T. Neff, C.A. Blau, Forced expression of cytidine deaminase confers resistance to cytosine arabinoside and gemcitabine, Exp. Hematol. 24 (1996) 1340–1346.

[8] C. Dumontet, K. Fabianowska-Majewska, D. Mantincic, E. Callet Bauchu, I. Tigaud, V. Gandhi, M. Lepoivre, G.J. Peters, M.O. Rolland, D. Wyczechowska, X. Fang, S. Gazzo, D.A. Voorn, A. Vanier-Viornery, J. MacKey, Common resistance mechanisms to deoxynucleoside analogues in variants of the human erythroleukaemic line K562, Br. J. Haematol. 106 (1999) 78–85.

[9] Y.G. Goan, B. Zhou, E. Hu, S. Mi, Y. Yen, Overexpression of ribonucleotide reductase as a mechanism of resistance to 2,2-difluorodeoxycytidine in the human KB cancer cell line, Cancer Res. 59 (1999) 4204–4207.

[10] C.M. Galmarini, M.L. Clarke, N. Falette, A. Puisieux, J.R. Mackey, C. Dumontet, Expression of a non-functional p53 affects the sensitivity of cancer cells to gemcitabine, Int. J. Cancer 97 (2002) 439–445.

[11] P.S. Moore, B. Sipos, S. Orlandini, C. Sorio, F.X. Real, N.R. Lemoine, T. Gress, C. Bassi, G. Kloppel, H. Kalthoff, H. Ungefroren, M. Lohr, A. Scarpa, Genetic profile of 22 pancreatic carcinoma cell lines. Analysis of K-ras, p53, p16 and DPC4/Smad4, Virchows Arch. 439 (2001) 798–802.

[12] M. Cascallo, J. Calbo, J.L. Gelpi, A. Mazo, Modulation of drug cytotoxicity by reintroduction of wild-type p53 gene (Ad5CMV-p53) in human pancreatic cancer, Cancer Gene Ther. 7 (2000) 545–556.

[13] M. Cascallo, J. Calbo, G. Capella, C. Fillat, M. Pastor-Anglada, A. Mazo, Enhancement of gemcitabine-induced apoptosis by restoration of p53 function in human pancreatic tumors, Oncology 68 (2005) 179–189.

[14] S. Maehara, S. Tanaka, M. Shimada, K. Shirabe, Y. Saito, K. Takahashi, Y. Maehara, Selenoprotein P, as a predictor for evaluating gemcitabine

resistance in human pancreatic cancer cells, Int. J. Cancer 112 (2004) 184–189.
[15] M. Ducasse, M.A. Brown, Epigenetic aberrations and cancer, Mol. Cancer 5 (2006) 60.
[16] P.A. Marks, M. Dokmanovic, Histone deacetylase inhibitors: discovery and development as anticancer agents, Expert Opin. Investig. Drugs 14 (2005) 1497–1511.
[17] M. Fournel, M.C. Trachy-Bourget, P.T. Yan, A. Kalita, C. Bonfils, C. Beaulieu, S. Frechette, S. Leit, E. Abou-Khalil, S.H. Woo, D. Delorme, A.R. MacLeod, J.M. Besterman, Z. Li, Sulfonamide anilides, a novel class of histone deacetylase inhibitors, are antiproliferative against human tumors, Cancer Res. 62 (2002) 4325–4330.
[18] A. Batova, L.E. Shao, M.B. Diccianni, A.L. Yu, T. Tanaka, A. Rephaeli, A. Nudelman, J. Yu, The histone deacetylase inhibitor AN-9 has selective toxicity to acute leukemia and drug-resistant primary leukemia and cancer cell lines, Blood 100 (2002) 3319–3324.
[19] C. Nervi, U. Borello, F. Fazi, V. Buffa, P.G. Pelicci, G. Cossu, Inhibition of histone deacetylase activity by trichostatin A modulates gene expression during mouse embryogenesis without apparent toxicity, Cancer Res. 61 (2001) 1247–1249.
[20] D.M. Vigushin, S. Ali, P.E. Pace, N. Mirsaidi, K. Ito, I. Adcock, R.C. Coombes, Trichostatin A is a histone deacetylase inhibitor with potent antitumor activity against breast cancer in vivo, Clin. Cancer Res. 7 (2001) 971–976.
[21] C. Henderson, M. Mizzau, G. Paroni, R. Maestro, C. Schneider, C. Brancolini, Role of caspases, Bid, and p53 in the apoptotic response triggered by histone deacetylase inhibitors trichostatin-A (TSA) and suberoylanilide hydroxamic acid (SAHA), J. Biol. Chem. 278 (2003) 12579–12589.
[22] H. Sawa, H. Murakami, Y. Ohshima, T. Sugino, T. Nakajyo, T. Kisanuki, Y. Tamura, A. Satone, W. Ide, I. Hashimoto, H. Kamada, Histone deacetylase inhibitors such as sodium butyrate and trichostatin A induce apoptosis through an increase of the bcl-2-related protein Bad, Brain Tumor Pathol. 18 (2001) 109–114.
[23] M. Donadelli, C. Costanzo, L. Faggioli, M.T. Scupoli, P.S. Moore, C. Bassi, A. Scarpa, M. Palmieri, Trichostatin A, an inhibitor of histone deacetylases, strongly suppresses growth of pancreatic adenocarcinoma cells, Mol. Carcinog. 38 (2003) 59–69.
[24] P.S. Moore, S. Barbi, M. Donadelli, C. Costanzo, C. Bassi, M. Palmieri, A. Scarpa, Gene expression profiling after treatment with the histone deacetylase inhibitor trichostatin A reveals altered expression of both pro- and anti-apoptotic genes in pancreatic adenocarcinoma cells, Biochim. Biophys. Acta 1693 (2004) 167–176.
[25] Y. Zhao, J. Tan, L. Zhuang, X. Jiang, E.T. Liu, Q. Yu, Inhibitors of histone deacetylases target the Rb-E2F1 pathway for apoptosis induction through activation of proapoptotic protein Bim, Proc. Natl. Acad. Sci. U. S. A. 102 (2005) 16090–16095.
[26] P. Piacentini, M. Donadelli, C. Costanzo, P.S. Moore, M. Palmieri, A. Scarpa, Trichostatin A enhances the response of chemotherapeutic agents in inhibiting pancreatic cancer cell proliferation, Virchows Arch. 448 (2006) 797–804.
[27] T.C. Chou, P. Talalay, Quantitative analysis of dose–effect relationships: the combined effects of multiple drugs or enzyme inhibitors, Adv. Enzyme Regul. 22 (1984) 27–55.
[28] F. Bruzzese, E. Di Gennaro, A. Avallone, S. Pepe, C. Arra, M. Caraglia, P. Tagliaferri, A. Budillon, Synergistic antitumor activity of epidermal growth factor receptor tyrosine kinase inhibitor gefitinib and IFN-alpha in head and neck cancer cells in vitro and in vivo, Clin. Cancer Res. 12 (2006) 617–625.
[29] J.K. Leach, G. Van Tuyle, P.S. Lin, R. Schmidt-Ullrich, R.B. Mikkelsen, Ionizing radiation-induced, mitochondria-dependent generation of reactive oxygen/nitrogen, Cancer Res. 61 (2001) 3894–3901.
[30] H. Puthalakath, A. Strasser, Keeping killers on a tight leash: transcriptional and post-translational control of the pro-apoptotic activity of BH3-only proteins, Cell Death Differ. 9 (2002) 505–512.
[31] M. Marani, T. Tenev, D. Hancock, J. Downward, N.R. Lemoine, Identification of novel isoforms of the BH3 domain protein Bim which directly activate Bax to trigger apoptosis, Mol. Cell. Biol. 22 (2002) 3577–3589.
[32] H. Pelicano, D. Carney, P. Huang, ROS stress in cancer cells and therapeutic implications, Drug Resist. Updat. 7 (2004) 97–110.
[33] M. Schirmer, A.P. Stegmann, F. Geisen, G. Konwalinka, Lack of cross-resistance with gemcitabine and cytarabine in cladribine-resistant HL60 cells with elevated 5′-nucleotidase activity, Exp. Hematol. 26 (1998) 1223–1228.
[34] B. Schniewind, M. Christgen, R. Kurdow, S. Haye, B. Kremer, H. Kalthoff, H. Ungefroren, Resistance of pancreatic cancer to gemcitabine treatment is dependent on mitochondria-mediated apoptosis, Int. J. Cancer 109 (2004) 182–188.
[35] X. Shi, S. Liu, J. Kleeff, H. Friess, M.W. Buchler, Acquired resistance of pancreatic cancer cells towards 5-Fluorouracil and gemcitabine is associated with altered expression of apoptosis-regulating genes, Oncology 62 (2002) 354–362.
[36] Z. Xu, H. Friess, M. Solioz, S. Aebi, M. Korc, J. Kleeff, M.W. Buchler, Bcl-x(L) antisense oligonucleotides induce apoptosis and increase sensitivity of pancreatic cancer cells to gemcitabine, Int. J. Cancer 94 (2001) 268–274.
[37] Z.W. Xu, H. Friess, M.W. Buchler, M. Solioz, Overexpression of Bax sensitizes human pancreatic cancer cells to apoptosis induced by chemotherapeutic agents, Cancer Chemother. Pharmacol. 49 (2002) 504–510.
[38] R. Chinery, J.A. Brockman, M.O. Peeler, Y. Shyr, R.D. Beauchamp, R.J. Coffey, Antioxidants enhance the cytotoxicity of chemotherapeutic agents in colorectal cancer: a p53-independent induction of p21WAF1/CIP1 via C/EBPbeta, Nat. Med. 3 (1997) 1233–1241.
[39] A. Laurent, C. Nicco, C. Chereau, C. Goulvestre, J. Alexandre, A. Alves, E. Levy, F. Goldwasser, Y. Panis, O. Soubrane, B. Weill, F. Batteux, Controlling tumor growth by modulating endogenous production of reactive oxygen species, Cancer Res. 65 (2005) 948–956.
[40] O. Ammerpohl, A. Trauzold, B. Schniewind, U. Griep, C. Pilarsky, R. Grutzmann, H.D. Saeger, O. Janssen, B. Sipos, G. Kloppel, H. Kalthoff, Complementary effects of HDAC inhibitor 4-PB on gap junction communication and cellular export mechanisms support restoration of chemosensitivity of PDAC cells, Br. J. Cancer 96 (2007) 73–81.
[41] N.B. Arnold, N. Arkus, J. Gunn, M. Korc, The histone deacetylase inhibitor suberoylanilide hydroxamic acid induces growth inhibition and enhances gemcitabine-induced cell death in pancreatic cancer, Clin. Cancer Res. 13 (2007) 18–26.
[42] C. Oliani, M. Padovani, P. Manno, D. Barana, M. Falconi, C. Bassi, G. Cavallini, P. Pederzoli, G.L. Cetto, Gemcitabine and continuous infusion of 5-fluorouracil in locally advanced and metastatic pancreatic cancer: a phase I–II study, Anticancer Res. 24 (2004) 2107–2112.
[43] J.D. Berlin, P. Catalano, J.P. Thomas, J.W. Kugler, D.G. Haller, A.B. Benson III, Phase III study of gemcitabine in combination with fluorouracil versus gemcitabine alone in patients with advanced pancreatic carcinoma: Eastern Cooperative Oncology Group Trial E2297, J. Clin. Oncol. 20 (2002) 3270–3275.
[44] M.G. Raraty, C.J. Magee, P. Ghaneh, J.P. Neoptolemos, New techniques and agents in the adjuvant therapy of pancreatic cancer, Acta Oncol. 41 (2002) 582–595.